

## Why Temperature Chaos in Spin Glasses Is Hard to Observe

T. Aspelmeier, A. J. Bray, and M. A. Moore

*Department of Physics and Astronomy, University of Manchester, Manchester M13 9PL, United Kingdom*

(Received 11 July 2002; published 17 October 2002)

The overlap length of a three-dimensional Ising spin glass on a cubic lattice with Gaussian interactions has been estimated numerically by transfer matrix methods and within a Migdal-Kadanoff renormalization group scheme. We find that the overlap length is large, explaining why it has been difficult to observe spin glass chaos in numerical simulations and experiment.

DOI: 10.1103/PhysRevLett.89.197202

PACS numbers: 75.50.Lk, 02.60.Pn, 75.10.Nr, 75.40.Mg

Chaos, rejuvenation, memory, and aging in spin glasses are currently being intensively studied [1–9]. “Chaos” refers to the property that equilibrium states in the ordered phase of spin glasses are sensitive to arbitrarily small changes in the couplings or in temperature, and is one possible explanation for memory effects in spin glasses [1], although other mechanisms are also present [5]. There is evidence both for and against temperature chaos in computer simulations: some authors claim to see the effects of chaos [8], and others have failed to see it [9,10]. In this Letter we start from the droplet [11] or scaling [12] pictures and calculate numerically the overlap length  $L^*(T, \Delta T)$ , i.e., the length scale beyond which spins at temperatures  $T$  and  $T + \Delta T$  become uncorrelated with each other, for a three-dimensional Edwards-Anderson Ising spin glass and also within a Migdal-Kadanoff renormalization group scheme (MKRG), both with a Gaussian distribution of couplings with unit variance. We show that this length scale is large within much of the parameter space, and only just comes down to magnitudes accessible to numerical simulations for certain values of  $T$  and  $\Delta T$ . We believe that this is why some workers have been unable to see chaos in their investigations. As a by-product, we will also find the root mean square droplet interface free energy  $F(T) \equiv \sqrt{\langle F_{\text{int}}^2(T) \rangle}$  and entropy  $S(T) \equiv \sqrt{\langle S_{\text{int}}^2(T) \rangle}$ . The angle brackets indicate averaging over realizations of the bond couplings. We show that  $S(T) \sim \sqrt{T}$  for small  $T$ , contrary to previous arguments [13].

In the MKRG scheme for three dimensions, renormalized bonds after  $n$  renormalization steps  $J^{(n)}$  are obtained from the set of bonds  $\{J^{(n-1)}\}$  after  $n - 1$  renormalization steps using the relation

$$\frac{J^{(n)}}{T} = \sum_{i=1}^4 \tanh^{-1} \left( \tanh \frac{J_{1i}^{(n-1)}}{T} \tanh \frac{J_{2i}^{(n-1)}}{T} \right), \quad (1)$$

where  $J_{1,2i}^{(n-1)}$  are randomly drawn members of the bond pool (“pool method”). For a detailed description of the method in the present context we refer the reader to [14]. The renormalized bonds play the role of the interface free energy of a system of linear size  $L = 2^n$ , to wit  $\frac{1}{2}F(T) =$

$\langle (J^{(n)})^2 \rangle^{1/2}$ , the angle brackets indicating the average over the bond pool. Similarly, the interface entropy is given by  $\frac{1}{2}S(T) = \lim_{\delta T \rightarrow 0} \langle (J^{(n)} - J'^{(n)})^2 \rangle^{1/2} / \delta T$ , where  $J'^{(n)}$  is the corresponding member of a bond pool which has been evolved at temperature  $T + \delta T$ .

The MKRG applied to chaos in spin glasses has the advantages that large length scales are easily accessible numerically and that it is possible to access and estimate the overlap length directly. Banavar and Bray [14] have shown that the overlap length  $L^*$  is related to the ratio of the interface entropy and interface free energy. Introducing the usual generalized stiffness coefficients  $Y(T)$  and  $\sigma(T)$  via

$$F(T) = Y(T)L^\theta \quad \text{and} \quad S(T) = \sigma(T)L^{d_s/2} \quad (2)$$

(valid for large system sizes  $L$ ), a measure of the overlap length for a temperature step  $\Delta T \ll T$  is obtained by equating  $F(T)$  and  $S(T)\Delta T$ :

$$L^* = \left( \frac{Y}{\sigma \Delta T} \right)^{1/\zeta}. \quad (3)$$

Here  $\zeta = \frac{d_s}{2} - \theta$  is the chaos exponent, where  $d_s$  is the fractal dimension of the droplet interface and  $\theta$  is the droplet excitation energy exponent.

Independently, the overlap length can be obtained as the length scale on which two initially identical bond pools  $\{J\}$  and  $\{J'\}$ , evolved at two different temperatures, decorrelate. A measure for this is  $L^* = 2^{n_0}$  where  $n_0$  is such that

$$\frac{\langle (J^{(n_0)} - J'^{(n_0)})^2 \rangle}{\langle (J^{(n_0)})^2 \rangle + \langle (J'^{(n_0)})^2 \rangle} = \frac{1}{2}. \quad (4)$$

This method does not require a small temperature difference. When the temperature difference does happen to be small, however, it agrees with the previous method up to a numerical factor close to unity (see below).

Repeating the numerical work from [14] with greater accuracy (pool size  $2 \times 10^6$  and “long double” precision) and for a larger set of temperatures, we find  $Y(T)$  and  $\sigma(T)$  as shown in Fig. 1. The data for  $\sigma(T)$  in this figure has been obtained using a fixed *relative* temperature change  $\epsilon = \delta T/T = 10^{-6}$  at each temperature.

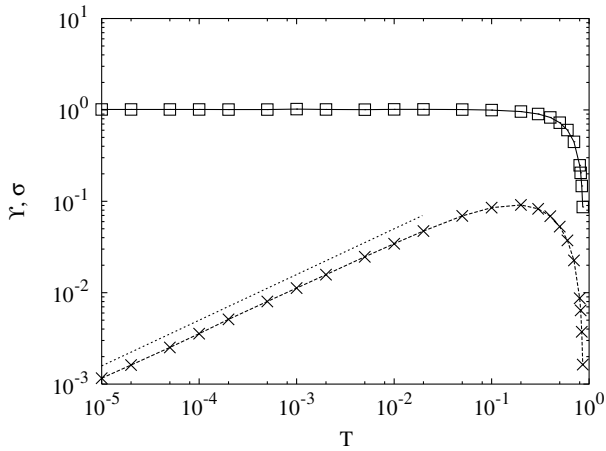


FIG. 1. Data for  $Y(T)$  (solid line) and  $\sigma(T)$  (dashed line) from Migdal-Kadanoff renormalization. The dotted line has slope  $1/2$  for comparison.

Huse and Fisher [13] argued that a droplet interface can be regarded as a collection of roughly independent two-level systems, each of which has on average an entropy proportional to  $T$ , which should give rise to  $S(T) \sim T$ . This is clearly violated by the data in Fig. 1. We will come back to this point later.

The overlap length  $L^*$  as obtained from the data for  $Y$  and  $\sigma$  using Eq. (3) is shown in Fig. 2. This requires knowing  $\zeta$ . For the  $d$ -dimensional Migdal-Kadanoff scheme,  $d_s = d - 1$  (i.e.,  $d_s = 2$  in the present case), and  $\theta$  was estimated from the numerics to be  $\theta = 0.25519 \pm 0.00005$  for  $d = 3$ ; therefore  $\zeta \approx 0.7448$ . For illustration, the temperature shift has been arbitrarily set to  $\Delta T = 0.01$  and  $\Delta T = 0.1$  for this plot. Since for these values of the parameters the temperature shift  $\Delta T$  is not much smaller than  $T$  for small  $T$ , Eq. (3) is not expected to hold and the “true” overlap length differs

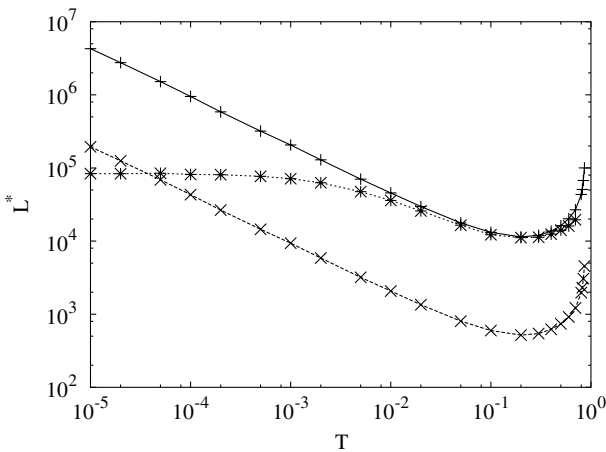


FIG. 2. Plot of the overlap length  $L^*$  as determined from the MKRG data and Eq. (3) with  $\zeta = 0.7448$  for  $\Delta T = 0.01$  (solid line) and  $\Delta T = 0.1$  (dashed line). The dotted line shows a direct determination of  $L^*$  for fixed absolute temperature shift  $\Delta T = 0.01$  (see text).

from the data shown. A direct determination of the overlap length (as the decorrelation length of the two bond pools as explained above) with  $\Delta T = 0.01$  is shown in Fig. 2 for comparison. A small constant has been added to the latter curve to make the two ways of determining  $L^*$  agree at the minimum. [This adjustment reflects the arbitrariness of the constant  $1/2$  in the definition, through Eq. (4), of  $L^*$ .] With this correction, the two curves for  $\Delta T = 0.01$  agree very well in a region around the minimum; they differ for small  $T$  since  $\Delta T \geq T$  and for  $T$  close to the critical temperature because of increasing influence of critical point controlled decorrelation [15].

Figure 3 shows a contour plot of the overlap length in the two-temperature plane, obtained from MKRG in the same manner as before. This figure shows that the overlap length is nowhere less than 40 for  $T_1, T_2 < T_c = 0.89645 \dots$ . Note that in agreement with [15] the overlap length is nonzero even above  $T_c$ .

Obviously,  $L^*$  is extraordinarily large for most values of  $T$  and never comes into a numerically accessible range, which, by today's standards, would be around  $L^* \approx 20$ .

While the Migdal-Kadanoff renormalization method allows the study of large length scales, it has drawbacks: the fractal dimension of a domain wall  $d_s$  on a cubic lattice is not well approximated, so the structure of an interface is significantly different on a hierarchical Berker lattice [16] (for which MKRG is exact) than on a cubic lattice. It is therefore not obvious that the overlap length as obtained above is characteristic of a three-dimensional Edwards-Anderson spin glass as well.

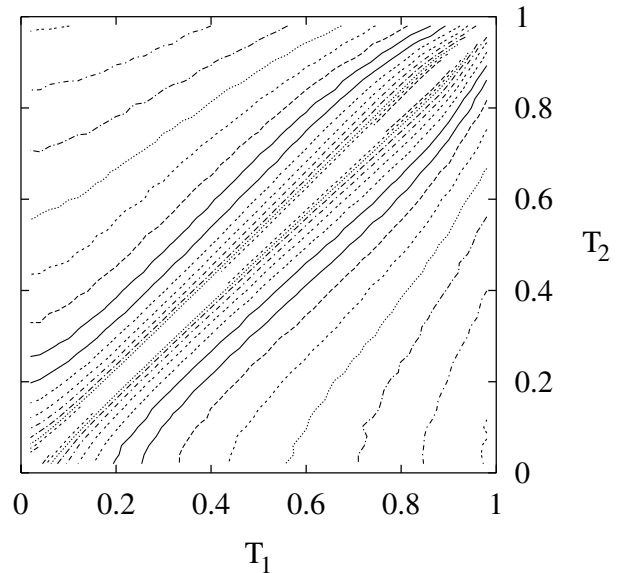


FIG. 3. The overlap length  $L^*$  as a function of two temperatures  $T_1$  and  $T_2$ . The contour lines are situated at  $L^* = 10^{n/5}$ , beginning with  $n = 8$  (i.e.,  $L^* \approx 40$  lattice spacings) and counting from the upper left and lower right hand corners towards the middle diagonal, where  $L^*$  diverges. The highest contour line shown is at  $n = 22$  where  $L^* \approx 25000$ .

In order to test this, we used the transfer matrix method as described in [17] to numerically obtain the interface free energy and entropy of small spin glass samples. This method has the disadvantage that due to demands on computer time and memory, only samples of size up to  $L = 4$  are accessible with reasonable statistics. On the positive side, there are no approximations involved whatsoever. This approach is therefore complimentary to the Migdal-Kadanoff scheme. We shall use Eq. (3), which applies generally wherever the droplet picture holds, to provide estimates of  $L^*$  from measurements of  $Y$  and  $\sigma$ .

The data for the interface free energy and entropy are shown in Fig. 4 as scaling plots for system sizes  $L = 2, 3, 4$ . The entropy has been obtained with a fixed relative temperature shift  $\epsilon = \delta T/T = 10^{-4}$ . The plot for  $F(T)$  allows for an estimate of  $\theta$ , the one for  $S(T)$  for an estimate of  $d_s$  [cf. Eq. (2)]. The values obtained are  $\theta \approx 0.18$  and  $d_s \approx 2.38$ , leading to  $\zeta \approx 1.01$ . While these numbers are merely crude estimates (corrections to scaling are expected to be significant for these small system sizes) and therefore no error bars have been supplied, they certainly lie in the expected range, and the value of  $d_s$ , in particular, shows that the droplet interface structure is much better captured even for these small systems than in the MKRG. The scaling in Fig. 4 naturally breaks down close to the critical temperature, due to the small system sizes.

The fractal dimension  $d_s$  can also be estimated at zero temperature from a bond perturbation calculation as in [12]. The result, shown in Fig. 5, is  $d_s \approx 2.7$ , obtained from sample sizes  $L = 2, 3, 4, 5$ . The discrepancy between this result and the one above illustrates the influence of finite size effects. A similar comparison in two dimensions [18], also shown in Fig. 5, gives the same kind of discrepancy for small  $L$ , which, however, is removed when going to larger  $L$ . It is found that the value obtained from bond perturbation is more reliable than the one obtained from a scaling plot of the entropy; the bond perturbation data lie almost perfectly on a straight line even down to  $L = 2$ . In three dimensions, the same seems to be true since  $d_s \approx 2.7$  compares well with  $d_s \approx 2.68$  from [19].

The interface entropy in Fig. 4 again scales as  $S(T) \sim \sqrt{T}$ , showing that this behavior is not special to the MKRG. In order to understand this, we modify the original two-level-system argument of [13]. The interface entropy is defined as the change in entropy after a change of boundary conditions. A two-level system which is not on the interface will have the same contribution to the *total* entropy under both boundary conditions, and therefore its contribution to the *interface* entropy cancels by taking the difference. A two-level system residing *on* the interface, however, will in general be in a different effective field under the two boundary conditions (since at least one, but not all of its neighboring spins have changed sign); therefore its excitation energy, and consequently its

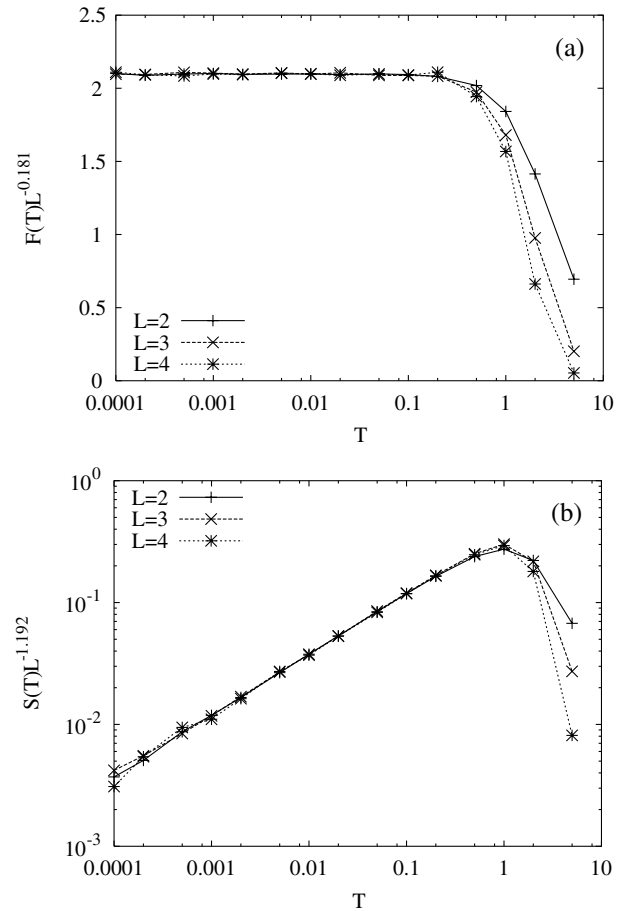


FIG. 4. Scaling plot for the interface free energy (top) and entropy (bottom). The numbers of samples used were  $2 \times 10^5$  ( $L = 2$ ),  $1 \times 10^5$  ( $L = 3$ ), and  $2 \times 10^4$  ( $L = 4$ ). With  $\theta = 0.181$  and  $d_s/2 = 1.192$  good data collapse is achieved.

contribution to the total entropy, will be different. This gives rise to a nonvanishing contribution to the interface entropy. Denoting the excitation energies under the two boundary conditions by  $\Delta^\pm$ , the interface entropy contribution from a two-level system on the interface is  $\Delta S(\Delta^+, \Delta^-) = S_{2\text{-lev}}(\Delta^+) - S_{2\text{-lev}}(\Delta^-)$ . It is easy to check that the entropy of a two-level system is

$$S_{2\text{-lev}}(\Delta) = \log\left(2 \cosh \frac{\Delta}{2T}\right) - \frac{\Delta}{2T} \tanh \frac{\Delta}{2T}. \quad (5)$$

The function  $S_{2\text{-lev}}(\Delta)$  has a maximum at  $\Delta = 0$  and decays to zero on scale  $T$ ; therefore  $\Delta S(\Delta^+, \Delta^-)$  is non-zero essentially only in two perpendicular strips of width  $T$  along the  $\Delta^\pm$  axes, excluding their overlap region around the origin. Thus only those two-level systems contribute to the interface entropy which have excitation energies  $\Delta^+ < T$  and  $\Delta^- > T$  (or vice versa). This implies that the second moment, taken with the joint probability distribution  $p(\Delta^+, \Delta^-)$ , goes as

$$\langle \Delta S^2 \rangle \sim \int_T^\infty d\Delta^+ \int_0^T d\Delta^- p(\Delta^+, \Delta^-) \sim T, \quad T \rightarrow 0,$$

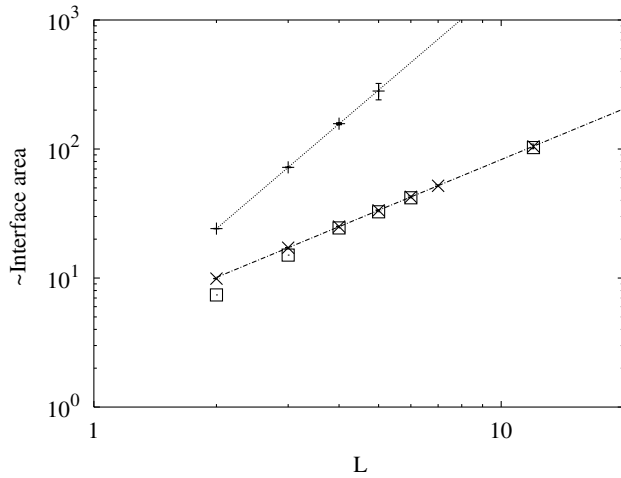


FIG. 5. Estimate of the interface area from a bond perturbation calculation. The + symbols are for  $d = 3$ , and the dashed straight line is a best fit with slope  $d_s = 2.697 \pm 0.002$ . The numbers of samples used are as in Fig. 4 and 100 for  $L = 5$ . The crosses are for  $d = 2$ , and the dotted straight line is a fit with  $d_s = 1.3$  (the line is to guide the eye only; better data can be found in [12]). The squares represent the average of  $S^2(T)/T$  in  $d = 2$  over a temperature range where this quantity is approximately constant, multiplied by an arbitrary number in order to make it comparable to the other data.

provided the marginal distribution  $\int_0^\infty d\Delta^+ p(\Delta^+, \Delta^-)$  is nonzero for  $\Delta^- = 0$ . This result is very well supported by the data in Figs. 1 and 4.

The overlap length as estimated from  $F(T)$ ,  $S(T)$ , and Eq. (3) is shown in Fig. 6. While being smaller than for the MKRG,  $L^*$  is still very large ( $L^* > 30$  for  $\Delta T < 0.1$ ) and thus (just) out of range of numerical simulations. In fact, with the parameters as used in [8] ( $T_1 = 0.7$ ,  $T_2 = 0.4$ ), the overlap length is estimated to be  $L^* \approx 20$ , while the authors are using a system of size  $L = 24$ . This is in accord with the authors' claim that they have been able to observe the effects of temperature chaos. Again, we would expect modifications to the small temperature behavior of  $L^*$  if a fixed absolute temperature shift is used (cf. Fig. 2), but not in the region of the minimum.

Finally, it is worth noting that the large value of the overlap length will have implications also for experiments on memory and rejuvenation. The effects of chaos are visible only when the length scale  $L(t)$  within which the spins are well-equilibrated after waiting for a time  $t$ , is larger than the overlap length  $L^*$ . As  $L(t)$  increases only very slowly with time, many experiments will not satisfy the criterion  $L(t) > L^*$ , and it will then be inappropriate to use chaos ideas to explain what is happening. In complete agreement with this, Jönsson *et al.* [7] have shown in two-temperature aging experiments on spin glasses that there is a crossover from accumulative aging [no chaos effects, i.e.  $L^* \gg L(t)$ ] to chaos-controlled aging [ $L^*$  comparable to  $L(t)$ ] when the temperature difference is increased.

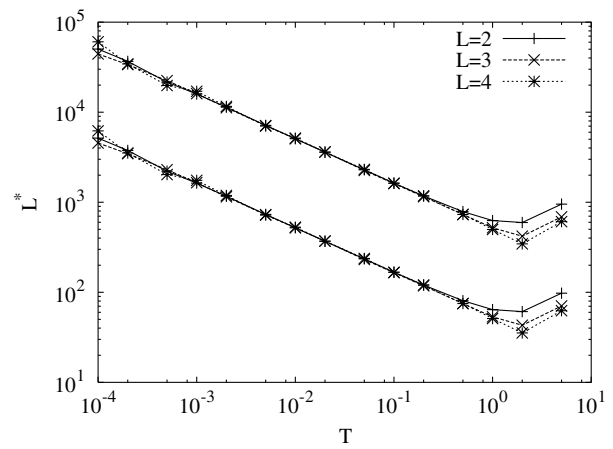


FIG. 6. Overlap length as calculated from the transfer matrix method. Top curves are for  $\Delta T = 0.01$ , bottom curves for  $\Delta T = 0.1$ . For this plot,  $\zeta = 1.01$  has been used as obtained from Fig. 4. There is no qualitative difference, however, if a more realistic  $\zeta = 1.15$  is used.

T. A. acknowledges support by the German Academic Exchange Service (DAAD).

- 
- [1] K. Jonason, E. Vincent, J. Hammann, J.-P. Bouchaud, and P. Nordblad, Phys. Rev. Lett. **81**, 3243 (1998).
  - [2] J.-P. Bouchaud, V. Dupuis, J. Hammann, and E. Vincent, Phys. Rev. B **65**, 024439 (2002).
  - [3] T. Rizzo, J. Phys. A **34**, 5531 (2001).
  - [4] H. Yoshino, A. Lemaître, and J.-P. Bouchaud, Eur. Phys. J. B **20**, 367 (2001).
  - [5] L. Berthier and J.-P. Bouchaud, cond-mat/0202069.
  - [6] F. Krzakala and O. C. Martin, cond-mat/203499.
  - [7] P. E. Jönsson, H. Yoshino, and P. Nordblad, Phys. Rev. Lett. **89**, 097201 (2002).
  - [8] H. Takayama and K. Hukushima, cond-mat/0205276.
  - [9] A. Billoire and E. Marinari, J. Phys. A **33**, L265 (2000).
  - [10] A. Billoire and E. Marinari, cond-mat/0202473.
  - [11] D. S. Fisher and D. A. Huse, Phys. Rev. Lett. **56**, 1601 (1986).
  - [12] A. J. Bray and M. A. Moore, Phys. Rev. Lett. **58**, 57 (1987).
  - [13] D. A. Huse and D. S. Fisher, Phys. Rev. Lett. **57**, 2203 (1986).
  - [14] J. R. Banavar and A. J. Bray, Phys. Rev. B **35**, 8888 (1987).
  - [15] M. Nifle and H. J. Hilhorst, Phys. Rev. Lett. **68**, 2992 (1992).
  - [16] A. N. Berker and S. Ostlund, J. Phys. C **12**, 4961 (1979).
  - [17] A. J. Bray and M. A. Moore, Phys. Rev. B **31**, 631 (1985).
  - [18] Since  $T_c = 0$  in two dimensions, the entropy scaling works only if  $L$  is much smaller than the correlation length, i.e., only at small temperatures.
  - [19] M. Palassini and A. P. Young, Phys. Rev. Lett. **83**, 5126 (1999).